



Cite this: *Chem. Sci.*, 2019, 10, 7076

All publication charges for this article have been paid for by the Royal Society of Chemistry

# Assembly of 1*H*-isoindole derivatives by selective carbon–nitrogen triple bond activation: access to aggregation-induced emission fluorophores for lipid droplet imaging†

Dandan He,<sup>a</sup> Zeyan Zhuang,<sup>b</sup> Xu Wang,<sup>a</sup> Jiawei Li,<sup>a</sup> Jianxiao Li,<sup>a</sup> Wanqing Wu,<sup>a,b</sup> Zujin Zhao,<sup>\*b</sup> Huanfeng Jiang<sup>ID</sup><sup>\*a</sup> and Ben Zhong Tang<sup>ID</sup><sup>bc</sup>

A novel strategy has been established to assemble a series of single (*Z*)- or (*E*)-1*H*-isoindole derivatives through selectively and sequentially activating carbon–nitrogen triple bonds in a multicomponent system containing various nucleophilic and electrophilic sites. The reaction provides efficient access to structurally unique fluorophores with aggregation-induced emission characteristics. These new fluorophores show fluorescence wavelengths and efficiencies that can be modulated and have excellent potential to specifically light up lipid droplets (LDs) in living cells with bright fluorescence, low cytotoxicity and better photostability than commercially available LD-specific dyes.

Received 1st March 2019  
Accepted 7th June 2019

DOI: 10.1039/c9sc01035a

rsc.li/chemical-science

## Introduction

Organic fluorophores are of significant interest in a wide range of disciplines on account of their promising applications in organic light-emitting diodes, chemical sensing and biological imaging.<sup>1</sup> Particularly, organic fluorophores containing *N*-heterocycles are highly desirable for organic chemistry research due to their ubiquity in biologically active natural products, organic functional materials and pharmaceuticals.<sup>2</sup> Over the past few decades, *N*-heterocycle-based fluorophores have been developed rapidly for biological imaging owing to their good biological activity.<sup>3,4</sup> Recently, some interesting fluorophores based on nitrogen-containing heterocycles which exhibit aggregation-induced emission (AIE) properties have been reported by the groups of Huang, Tian, Liu and us.<sup>5,6</sup> Thanks to the AIE effect, these fluorophores are free of aggregation-caused emission quenching, and can fluoresce strongly in the aggregated state, such as nanoparticles, which enables them to perform efficiently in tracking various organelles in living cells *via* fluorescence imaging techniques. To facilitate the

advancement in this field, novel design and direct synthesis of new fluorophores containing *N*-heterocycles are highly demanded.

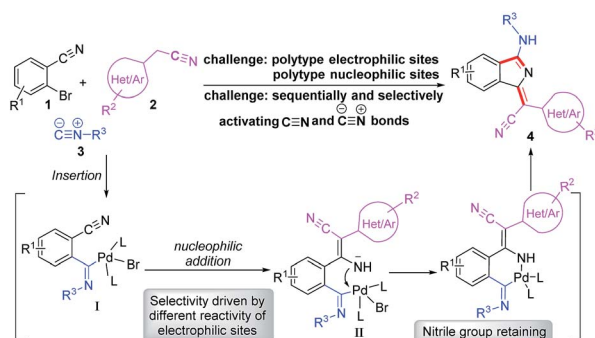
It is known that the molecular structure determines the properties, and the control and modification of the structure would endow materials with different properties.<sup>7</sup> Developing efficient and selective synthetic methods is key to construct various new skeletons. For research concerning precise creation and controlled synthesis of functional molecules, traditional chemistry faces challenges of increasing systematicness and comprehensiveness. Consequently, the design, synthesis and discovery of properties of functional molecules are undoubtedly a tendency of organic chemistry. Given the importance of elemental nitrogen in functional materials, it can be expected that when introducing multiple nitrogen atoms or various nitrogen-containing groups into the target molecules, novel properties should be obtained. Nitriles are common platform

<sup>a</sup>Key Laboratory of Functional Molecular Engineering of Guang Dong Province, School of Chemistry and Chemical Engineering, South China University of Technology, Guangzhou 510641, P. R. China. E-mail: cewuq@scut.edu.cn; jianghf@scut.edu.cn

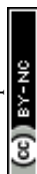
<sup>b</sup>State Key Laboratory of Luminescent Materials and Devices, Center for Aggregation-Induced Emission, South China University of Technology, Guangzhou 510640, China. E-mail: mszjzhao@scut.edu.cn

<sup>c</sup>Department of Chemistry, Hong Kong Branch of Chinese National Engineering Research Center for Tissue Restoration and Reconstruction, The Hong Kong University of Science & Technology, Kowloon, Hong Kong, China

† Electronic supplementary information (ESI) available. CCDC 1868897, 1880913, 1880930 and 1869980. For ESI and crystallographic data in CIF or other electronic format see DOI: 10.1039/c9sc01035a



Scheme 1 Proposed synthetic route for 1*H*-isoindole derivatives.



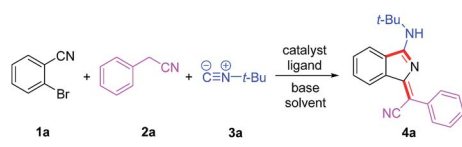
chemicals in the chemical commodity industry, and the low cost coupled with versatile transformation of these molecules underlies their great use in industrial and academic communities. For instance, nitriles may serve as a valuable precursor toward structurally diverse compounds such as amines,<sup>8</sup> amides,<sup>9</sup> ketones,<sup>10</sup> and heterocycles.<sup>11</sup> In most cases, however, nitriles are used as solvents or ligands in organometallic reactions,<sup>12</sup> presumably due to the inherently inert nature of carbon–nitrogen triple bonds. To address this issue, many methods for activating nitriles have been reported recently. Generally, three strategies for nitrile transformation are typically employed: (i) nucleophilic addition reaction,<sup>13</sup> (ii) electrophilic addition reaction,<sup>14</sup> and (iii) radical addition reaction.<sup>15</sup> Despite recent advances in carbon–nitrogen triple bond transformation,<sup>16</sup> a selective and sequential activation of carbon–nitrogen triple bonds is yet to be realized.

Based on our previous work, we anticipate that a convenient and concise approach to assemble a series of carbon–nitrogen triple bonds with different activities could be provided by rational design. As illustrated in the proposed synthetic route (Scheme 1), isocyanide **3** is initially activated *via* an insertion reaction to give intermediate **I**. Subsequently, the nucleophilic addition of **2** to the nitrile group of **I** forms intermediate **II**, which is selectively driven by different reactivities of electrophilic sites. Finally, the desired 1*H*-isoindole product **4** would be obtained through the reductive elimination and isomerization of **II**. This protocol, a palladium-catalyzed multicomponent cross-coupling reaction, provides direct access to novel fluorescent scaffolds with desirable potential properties. Moreover, the photophysical properties and potential bioimaging application of the synthesized 1*H*-isoindole derivatives can be further investigated.

## Results and discussion

We commenced our study by optimizing reaction conditions with 2-bromobenzonitrile (**1a**), 2-phenylacetonitrile (**2a**) and *tert*-butyl isocyanide (**3a**) as model substrates. Initially, the feasibility

Table 1 Optimization of reaction conditions<sup>a</sup>

|  |                      |                               |                                 |         |                        |
|--|----------------------|-------------------------------|---------------------------------|---------|------------------------|
| Entry <sup>a</sup>   | [Pd]                 | Ligand                        | Base                            | Solvent | Yield <sup>b</sup> (%) |
| 1  | Pd(OAc) <sub>2</sub> | PPh <sub>3</sub>              | <i>t</i> -BuOK                  | DMSO    | 51                     |
| 2  | Pd(OAc) <sub>2</sub> | PPh <sub>3</sub>              | <i>t</i> -BuONa                 | DMSO    | n.d.                   |
| 3  | Pd(OAc) <sub>2</sub> | PPh <sub>3</sub>              | Cs <sub>2</sub> CO <sub>3</sub> | DMSO    | n.d.                   |
| 4  | PdCl <sub>2</sub>    | PPh <sub>3</sub>              | <i>t</i> -BuOK                  | DMSO    | 28                     |
| 5  | Pd(TFA) <sub>2</sub> | PPh <sub>3</sub>              | <i>t</i> -BuOK                  | DMSO    | Trace                  |
| 6  | Pd(OAc) <sub>2</sub> | PPh <sub>3</sub>              | <i>t</i> -BuOK                  | Dioxane | 48                     |
| 7  | Pd(OAc) <sub>2</sub> | PPh <sub>3</sub>              | <i>t</i> -BuOK                  | DMF     | Trace                  |
| 8  | Pd(OAc) <sub>2</sub> | L1                            | <i>t</i> -BuOK                  | DMSO    | Trace                  |
| 9  | Pd(OAc) <sub>2</sub> | P( <i>t</i> -Bu) <sub>3</sub> | <i>t</i> -BuOK                  | DMSO    | Trace                  |
| 10   | Pd(OAc) <sub>2</sub> | L2                            | <i>t</i> -BuOK                  | DMSO    | 38                     |
| 11 <sup>c</sup>  | Pd(OAc) <sub>2</sub> | PPh <sub>3</sub>              | <i>t</i> -BuOK                  | DMSO    | 67                     |
| 12 <sup>d</sup>  | Pd(OAc) <sub>2</sub> | PPh <sub>3</sub>              | <i>t</i> -BuOK                  | DMSO    | 81 (79)                |

<sup>a</sup> All reactions were performed with **1a** (0.2 mmol), **2a** (1 equiv.), **3a** (1 equiv.), palladium catalyst (10 mol%), ligand (20 mol%), base (3 equiv.), and solvent (1 mL), at 120 °C under air for 12 h. <sup>b</sup> The yield was determined by GC with *n*-dodecane as the internal standard based on **1a**. n.d. = not determined. <sup>c</sup> **2a** (2 equiv.) and **3a** (2 equiv.). <sup>d</sup> **2a** (2 equiv.), **3a** (2 equiv.), and dry DMSO. L1: tri-*o*-tolylphosphine. L2: thiosemicarbazide.

of the hypothesis was confirmed by product **4a** obtained in 51% yield when the reaction was treated with 10 mol% Pd(OAc)<sub>2</sub>, 20 mol% PPh<sub>3</sub> and 3 equivalents of *t*-BuOK in 1 mL DMSO at 120 °C for 12 h under air (Table 1, entry 1). Encouraged by this observation, further study of other reaction parameters was carried out. The examination of different bases revealed that *t*-BuOK was the most appropriate choice (Table 1, entries 2 and 3). Subsequent screening of catalysts showed that Pd(OAc)<sub>2</sub> still gave the best result (Table 1, entries 4 and 5). In addition, a series of ligands and solvents were tested (Table 1, entries 6–10) and the highest yield (79%) of **4a** was attributed to the increased equivalents of **2a** and **3a** in dry DMSO (Table 1, entry 12). The

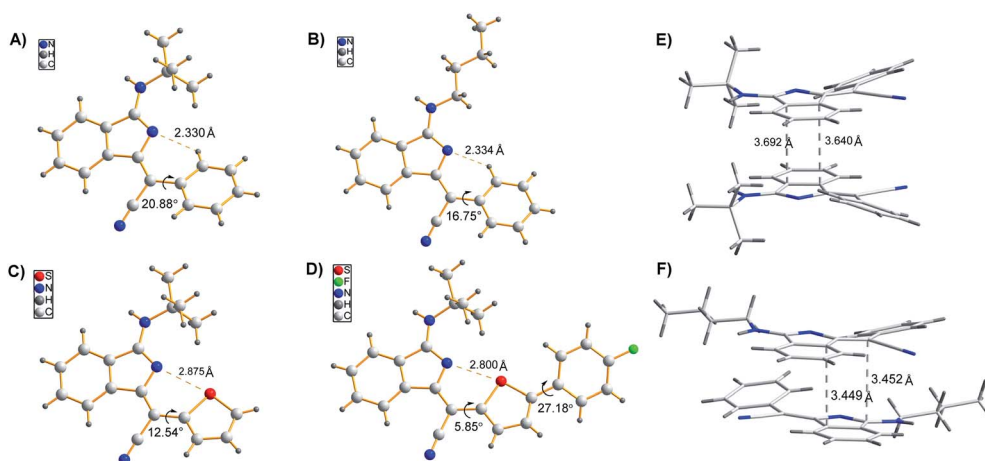
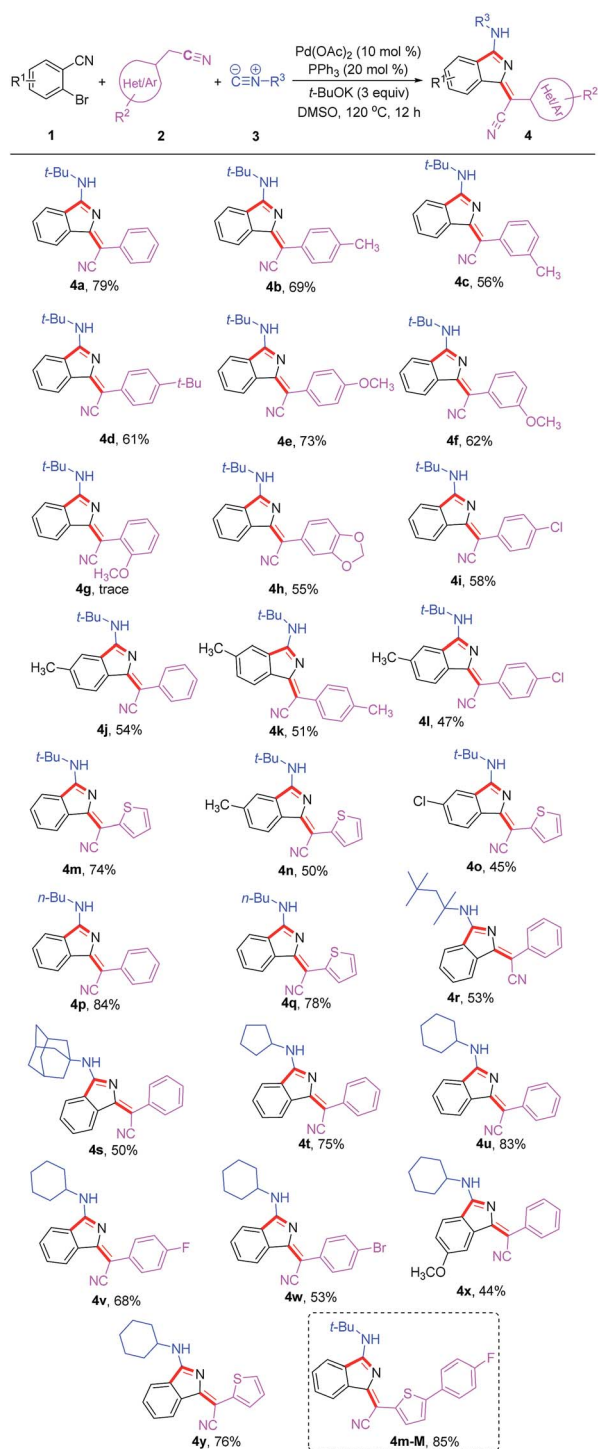


Fig. 1 (A–D) Single crystal structures of **4a**, **4p**, **4m**, and **4m-M**. (E and F) Molecular packing of **4a** (A) and **4p** (B) in crystals.



Table 2 Substrate scope<sup>a</sup>

<sup>a</sup> Reaction conditions: all reactions were performed with **1** (0.2 mmol), **2** (2 equiv.), **3** (2 equiv.), Pd(OAc)<sub>2</sub> (10 mol%), PPh<sub>3</sub> (20 mol%), *t*-BuOK (3 equiv.), and dry DMSO (1 mL), at 120 °C under air for 12 h.

structure and configuration of 1*H*-isoindoles were confirmed by X-ray crystal analysis (Fig. 1).<sup>17</sup> The single *E* configuration of the carbon–carbon double bond in compound **4a** could be explained by intramolecular C–H⋯N hydrogen

bonding, which will effectively rigidify the molecular structure and increase the stability of the molecule (Fig. 1A).

Under the optimized conditions, the substrate scope was then explored (Table 2). Diversely substituted acetonitriles were employed as the substrates. Both electron-donating (OMe, *t*-Bu and Me) and electron-withdrawing (F, Cl and Br) groups in 2-phenylacetonitriles were compatible and the corresponding products were afforded in 53–73% yields. Notably, when using 2-thiopheneacetonitrile as the substrate, the corresponding products **4m** and **4y** were isolated in good yields of 74% and 76%, respectively. In addition, other tested alkyl isocyanides such as *n*-butyl isocyanide, 1,1,3,3-tetramethylbutyl isocyanide, adamantyl isocyanide, cyclopentyl isocyanide and cyclohexyl isocyanide were found to be suitable for this transformation, converting to the corresponding products **4p–4y** in 44–84% yields. Additionally, the reactions of 2-bromobenzonitriles with different functional groups also proceeded smoothly under the standard conditions to deliver products **4j**, **4o** and **4x** in acceptable yields. The good functional group compatibility, especially for the thiophene group, could be conveniently modified for the purpose of fluorescence–structure relationship study. Compound **4m–M** containing an extended conjugation system could be constructed easily from **4m** in 85% yield *via* bromination and Suzuki coupling reaction.

To demonstrate the potential application of this method, the photophysical properties of these synthetic fluorophores were carefully investigated (Tables 3 and S1†). 1*H*-isoindoles derivatives, which were converted from 2-phenylacetonitriles with different functional groups, show similar absorption maxima in the range of 392–415 nm in CH<sub>2</sub>Cl<sub>2</sub> solution. They emit very weak fluorescence in solutions with extremely low fluorescence quantum yields ( $\Phi_F$ s) of 0.2–0.9%, but exhibit intense fluorescence in the range of 408–438 nm with a much higher  $\Phi_F$ s of 1.9–26.3% in solid films, demonstrating AIE characteristics, which was further confirmed from the emission spectra of **4a** in water/methanol with different water fractions (Fig. S1†). For these new AIE fluorophores, the intramolecular motion of flexible rotors (*e.g.* the aromatic rings linked with *R*<sup>2</sup>) accounts for the quenching of fluorescence in the solution state, while the restriction of such a kind of motion results in emission enhancement in the aggregated state.<sup>18</sup> Besides, the efficient fluorescence in the aggregated state is also attributed to the bulky *R*<sup>3</sup> fragment, which suppresses close packing and thus strong intermolecular interactions.<sup>19</sup> In other words, the solid-state fluorescence behaviours can be well modulated by changing *R*<sup>3</sup>. As shown in Fig. 1, compared to **4p** with a normal butyl group, **4a** bearing a bulkier tertiary butyl group adopts a looser packing mode in crystals to avoid close  $\pi$ – $\pi$  stacking, leading to a higher  $\Phi_F$ s for **4a** than **4p** in both film and powder. Moreover, the fluorescence wavelength could be further tuned by utilizing substrates **2** with different functional groups. For instance, **4m** shows a yellow fluorescence peak at 553 nm in film, which is apparently red-shifted relative to the green fluorescence of **4a** (518 nm) and **4p** (526 nm). This can be ascribed to the strengthened electron donor–acceptor interaction when electron-donating thiophene is introduced.<sup>20</sup> In addition,



Table 3 Photophysical properties of representative 1*H*-isindole derivatives

| Compound    | $\lambda_{\text{abs}}$ (nm) <sup>a</sup>  |                      | $\lambda_{\text{em}}$ (nm) <sup>e</sup> |    | Stokes shift (cm <sup>-1</sup> ) <sup>f</sup> | $\Phi_{\text{F}}^g$ (%)            |         |           |
|-------------|---|----------------------|---|----|---|------------------------------------|---------|-----------|
|             | In CH <sub>2</sub> Cl <sub>2</sub> <sup>b</sup> ( $\epsilon$ (10 <sup>4</sup> M <sup>-1</sup> cm <sup>-1</sup> ) <sup>c</sup> ) | In film <sup>d</sup> | In film                                 |    |   | In CH <sub>2</sub> Cl <sub>2</sub> | In film | In powder |
| <b>4a</b>   | 394 (1.76)  | 411                  | 518                                     | 50 |   | 0.2                                | 25.0    | 33.8      |
| <b>4m</b>   | 423 (3.44)  | 431                  | 553                                     | 51 |   | 0.5                                | 2.7     | 16.4      |
| <b>4p</b>   | 396 (2.27)  | 423                  | 526                                     | 46 |   | 0.6                                | 13.5    | 21.0      |
| <b>4m-M</b> | 453 (3.17)  | 456                  | 589                                     | 50 |   | 0.9                                | 2.6     | 8.0       |

<sup>a</sup> Maximum absorption wavelength. <sup>b</sup> Measured in CH<sub>2</sub>Cl<sub>2</sub> at 10.0  $\mu\text{M}$ . <sup>c</sup> Molar absorption coefficient. <sup>d</sup> Measured in a drop-cast film on a quartz plate. <sup>e</sup> Emission peak (excited using the maximum absorption wavelength in CH<sub>2</sub>Cl<sub>2</sub> as the excitation wavelength). <sup>f</sup> Stokes shift =  $1/\lambda_{\text{abs}}$  (in film) –  $1/\lambda_{\text{em}}$  (in film). <sup>g</sup> Absolute fluorescence quantum yield measured by calibrated integration.

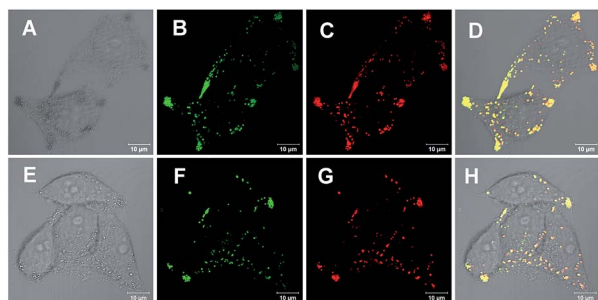


Fig. 2 Co-localization experiments of HeLa cells pretreated with oleic acid and stained with 5  $\mu\text{M}$  **4a** or **4m-M** for 15 min and then co-stained with a 1 : 1000 dilution of HCS LipidTOX<sup>TM</sup> Deep Red neutral lipid stain: (A and E) bright-field images, (B and F) images from **4a** and **4m-M** on channel 1 (**4a**:  $\lambda_{\text{ex}}$  = 405,  $\lambda_{\text{em}}$  = 450–570; **4m-M**:  $\lambda_{\text{ex}}$  = 405,  $\lambda_{\text{em}}$  = 480–600), (C and G) images from HCS LipidTOX<sup>TM</sup> Deep Red neutral lipid stain on channel 2 ( $\lambda_{\text{ex}}$  = 633,  $\lambda_{\text{em}}$  = 640–740), and (D and H) merged images from A–C and E–G, respectively.

containing a more extended conjugation system, **4m-M** can emit orange light at 589 nm.

With an AIE fluorophore library in hand, compound **4a** and modified **4m-M** were selected as fluorescent probes for live cell imaging. Lipid droplets (LDs) are uniquely encapsulated by a phospholipid monolayer, which segregates their hydrophobic neutral lipid core from the aqueous cytosol.<sup>21</sup> Considering the lipophilic properties of the fluorophores used, we tried to perform hydrophobic LD localization experiments with HeLa cells. Cell image data were obtained *via* irradiation at 405 nm on HeLa cells co-stained with **4a** or **4m-M** and HCS LipidTOX<sup>TM</sup> Deep Red neutral lipid stain, a commercial probe enabling the differentiation of LDs from other organelles. As shown in Fig. 2, the merged images, with high overlap ratios (88% and 84% respectively), indicate the excellent specific targeting ability of **4a** and **4m-M** toward LDs in living cells.

The photostability, as an important evaluation criterion for fluorescence probes, was measured quantitatively together with three commercially available LD-specific dyes, BODIPY, Nile red and HCS LipidTOX<sup>TM</sup> Deep Red neutral lipid stain. After exposure to a 405 nm laser with a power of 10% (3 mW) for 10 s between every scan interval for 30 scans, the fluorescence signal intensity of three commercial trackers was drastically lost, even Nile red was reduced to less than 20% of its initial

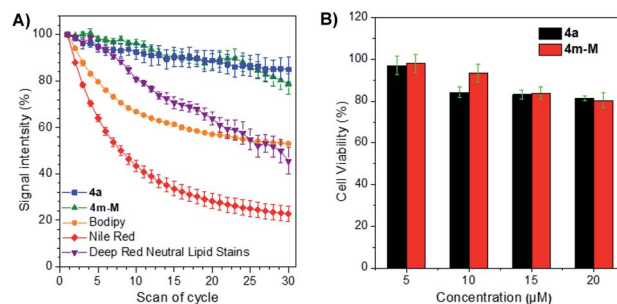


Fig. 3 (A) Photobleaching experiment: the signal intensity changed in HeLa cells stained with 5  $\mu\text{M}$  **4a**, **4m-M**, BODIPY or Nile red or a 1 : 1000 dilution of HCS LipidTOX<sup>TM</sup> Deep Red neutral lipid stain upon continuous scanning (the cells were exposed to 405 nm with 10% powder (3 mW) for 10 s in every interval). (B) Cell viability of HeLa cells after incubation with different concentrations of **4a** or **4m-M** (5, 10, 15 and 20  $\mu\text{M}$  of **4a** or **4m-M**) for 24 h.

value, while approximately 80% of the signal intensity of **4a** and **4m-M** was retained under the same conditions (Fig. 3A). The result suggests that the two fluorophores have excellent photostability, while BODIPY, Nile red and HCS LipidTOX<sup>TM</sup> Deep Red neutral lipid stain suffer from serious photobleaching. In addition, based on 3-(4,5-dimethyl-2-thiazolyl)-2,5-diphenyltetrazolium bromide (MTT) assay, we also evaluated the cytotoxicity of the two fluorophores by using them to incubate HeLa cells. As presented in Fig. 3B, a negligible change in HeLa cell viability was observed even when 20  $\mu\text{M}$  **4a** or **4m-M** was added to the culture medium for 24 h, which indicated that the two fluorophores have good biocompatibility to living cells.

## Conclusions

In conclusion, we have developed a highly stereoselective Pd-catalyzed cross-coupling reaction to access a library of AIE fluorophores, 1*H*-isindole derivatives, by selective carbon–nitrogen triple bond activation. The system exhibits several impressive characteristics including single *Z* or *E* selectivity, simple and diverse structures, and tunable and bright fluorescence. These AIE fluorophores have been proven to be considerably efficient reagents for cell imaging, which show excellent LD-targeting specificity and much higher photostability than



commercial LD-staining dyes. The protocol should provide a new strategy for the systematic study of the design, synthesis and discovering new specific properties of functional molecules.

## Conflicts of interest

There are no conflicts to declare.

## Acknowledgements

The authors thank the National Key Research and Development Program of China (2016YFA0602900), the National Natural Science Foundation of China (21490572 and 21672072), the Guangdong Natural Science Foundation (2018B030308007), and the Pearl River S&T Nova Program of Guangzhou (201610010160) for financial support.

## Notes and references

- (a) L. Yuan, W. Lin, K. Zheng, L. He and W. Huang, *Chem. Soc. Rev.*, 2013, **42**, 622; (b) X. Li, X. Gao, W. Shi and H. Ma, *Chem. Rev.*, 2014, **114**, 590; (c) S. W. Yun, N. Y. Kang, S. J. Park, H. H. Ha, Y. K. Kim, J. S. Lee and Y.-T. Chang, *Acc. Chem. Res.*, 2014, **47**, 1277; (d) Z. Yang, A. Sharma, J. Qi, X. Peng, D. Y. Lee, R. Hu, D. Lin, J. Qu and J. S. Kim, *Chem. Soc. Rev.*, 2016, **45**, 4651; (e) V. Fernández-Luna, P. D. Coto and R. D. Costa, *Angew. Chem., Int. Ed.*, 2018, **57**, 8826; (f) J. Tagare and S. Vaidyanathan, *J. Mater. Chem. C*, 2018, **6**, 10138.
- Y. Jiang, K. Xu and C. Zeng, *Chem. Rev.*, 2018, **118**, 4485.
- (a) K. Tikhomirova, A. Anisimov and A. Khoroshutin, *Eur. J. Org. Chem.*, 2012, 2201; (b) B. Liu, Z. Wang, N. Wu, M. Li, J. You and J. Lan, *Chem.-Eur. J.*, 2012, **18**, 1599; (c) S. Takahashi, Y. Kagami, K. Hanaoka, T. Terai, T. Komatsu, T. Ueno, M. Uchiyama, I. Koyama-Honda, N. Mizushima, T. Taguchi, H. Arai, T. Nagano and Y. Urano, *J. Am. Chem. Soc.*, 2018, **140**, 5925; (d) Y. Cheng, G. Li, Y. Liu, Y. Shi, G. Gao, D. Wu, J. Lan and J. You, *J. Am. Chem. Soc.*, 2016, **138**, 4730; (e) J. A. González-Vera, F. Fueyo-González, I. Alkorta, M. Peyressatre, M. C. Morris and R. Herranz, *Chem. Commun.*, 2016, **52**, 9652; (f) F. D. Moliner, N. Kielland, R. Lavilla and M. Vendrell, *Angew. Chem., Int. Ed.*, 2017, **56**, 3758; (g) A. C. Shaikh, D. S. Ranade, P. R. Rajamohanan, P. P. Kulkarni and N. T. Patil, *Angew. Chem., Int. Ed.*, 2017, **56**, 757; (h) Y. Chen, W. Zhang, Z. Zhao, Y. Cai, J. Gong, R. T. K. Kwok, J. W. Y. Lam, H. H. Y. Sung, I. D. Williams and B. Z. Tang, *Angew. Chem., Int. Ed.*, 2018, **57**, 5011; (i) J. Ohata, M. K. Miller, C. M. Mountain, F. Vohidov and Z. T. Ball, *Angew. Chem., Int. Ed.*, 2018, **57**, 2827.
- (a) A. L. Odom and T. J. McDaniel, *Acc. Chem. Res.*, 2015, **48**, 2822; (b) J. Xuan and A. Studer, *Chem. Soc. Rev.*, 2017, **46**, 4329.
- J. Luo, Z. Xie, J. W. Y. Lam, L. Cheng, H. Chen, C. Qiu, H. S. Kwok, X. Zhan, Y. Liu, D. Zhu and B. Z. Tang, *Chem. Commun.*, 2001, 1740.
- (a) J. Mei, N. L. C. Leung, R. T. K. Kwok, J. W. Y. Lam and B. Z. Tang, *Chem. Rev.*, 2015, **115**, 11718; (b) G. Yu, D. Wu, Y. Li, Z. Zhang, L. Shao, J. Zhou, Q. Hu, G. Tang and F. Huang, *Chem. Sci.*, 2016, **7**, 3017; (c) J. Mei, Y. Huang and H. Tian, *ACS Appl. Mater. Interfaces*, 2018, **10**, 12217; (d) F. Hu, X. Cai, P. N. Manghnani, Kenry, W. Wu and B. Liu, *Chem. Sci.*, 2018, **9**, 2756.
- (a) J. H. Kim, T. Gensch, D. Zhao, L. Stegemann, C. A. Strassert and F. Glorius, *Angew. Chem., Int. Ed.*, 2015, **54**, 10975; (b) H. Lu, Y. Zheng, X. Zhao, L. Wang, S. Ma, X. Han, B. Xu, W. Tian and H. Gao, *Angew. Chem., Int. Ed.*, 2016, **55**, 155; (c) S. Sasaki, S. Suzuki, W. M. C. Sameera, K. Igawa, K. Morokuma and G. Konishi, *J. Am. Chem. Soc.*, 2016, **138**, 8194; (d) B. Tang, C. Wang, Y. Wang and H. Zhang, *Angew. Chem., Int. Ed.*, 2017, **56**, 12543.
- (a) J.-B. Feng and X.-F. Wu, *Adv. Synth. Catal.*, 2016, **358**, 2179; (b) S. Chakraborty, G. Leitus and D. Milstein, *Chem. Commun.*, 2016, **52**, 1812; (c) X. Zhang, X. Xie and Y. Liu, *Chem. Sci.*, 2016, **7**, 5815; (d) M. Xiong, X. Xie and Y. Liu, *Org. Lett.*, 2017, **19**, 3398; (e) X. Yang, H. Yu, Y. Xu and L. Shao, *J. Org. Chem.*, 2018, **83**, 9682.
- (a) G. C. Midya, A. Kapat, S. Maiti and J. Dash, *J. Org. Chem.*, 2015, **80**, 4148; (b) P. Marcé, J. Lynch, J. Blackerby and J. M. J. Williams, *Chem. Commun.*, 2016, **52**, 1436; (c) Y. Li, H. Chen, J. Liu, X. Wan and Q. Xu, *Green Chem.*, 2016, **18**, 4865.
- (a) C. Zhou and R. C. Larock, *J. Am. Chem. Soc.*, 2004, **126**, 2302; (b) J. Lindh, P. J. R. Sjöberg and M. Larhed, *Angew. Chem., Int. Ed.*, 2010, **49**, 7733; (c) T. Miao and G.-W. Wang, *Chem. Commun.*, 2011, **47**, 9501; (d) J.-C. Hsieh, Y.-C. Chen, A.-Y. Cheng and H.-C. Tseng, *Org. Lett.*, 2012, **14**, 1282; (e) M. Meng, L. Yang, K. Cheng and C. Qi, *J. Org. Chem.*, 2018, **83**, 3275; (f) J. Zhang, F. Zhang, L. Lai, J. Cheng, J. Sun and J. Wu, *Chem. Commun.*, 2018, **54**, 3891.
- (a) M. Ramanathan and S.-T. Liu, *J. Org. Chem.*, 2015, **80**, 5329; (b) Y.-L. Chen, P. Sharma and R.-S. Liu, *Chem. Commun.*, 2016, **52**, 3187; (c) R.-R. Zhou, Q. Cai, D.-K. Li, S.-Y. Zhuang, Y.-W. Wu and A.-X. Wu, *J. Org. Chem.*, 2017, **82**, 6450; (d) M. Ramanathan, Y.-H. Liu, S.-M. Peng and S.-T. Liu, *Org. Lett.*, 2017, **19**, 5840; (e) M. Ramanathan and S.-T. Liu, *J. Org. Chem.*, 2017, **82**, 8290; (f) U. T. Das, L. J. W. Shimon and D. Milstein, *Chem. Commun.*, 2017, **53**, 13133; (g) S. Yao, K. Zhou, J. Wang, H. Cao, L. Yu, J. Wu, P. Qiu and Q. Xu, *Green Chem.*, 2017, **19**, 2945; (h) K. T. Ashitha, V. P. Kumar, C. T. F. Salfeena and B. S. Sasidhar, *J. Org. Chem.*, 2018, **83**, 113; (i) X. Yu, L. Gao, L. Jia, Y. Yamamoto and M. Bao, *J. Org. Chem.*, 2018, **83**, 10352; (j) A. Kishi, K. Moriyama and H. Togo, *J. Org. Chem.*, 2018, **83**, 11080; (k) M. Ramanathan and S.-T. Liu, *J. Org. Chem.*, 2018, **83**, 14138; (l) L. Su, K. Sun, N. Pan, L. Liu, M. Sun, J. Dong, Y. Zhou and S.-F. Yin, *Org. Lett.*, 2018, **20**, 3399; (m) Y. Zhang, Y. Shao, J. Gong, K. Hu, T. Cheng and J. Chen, *Adv. Synth. Catal.*, 2018, **360**, 3260.
- (a) F. F. Fleming and Q. Wang, *Chem. Rev.*, 2003, **103**, 2035; (b) S. F. Rach and F. E. Kühn, *Chem. Rev.*, 2009, **109**, 2061.



- 13 (a) S. Huang, Y. Shao, L. Zhang and X. Zhou, *Angew. Chem., Int. Ed.*, 2015, **54**, 14452; (b) F. Xue and T. Hayashi, *Angew. Chem., Int. Ed.*, 2018, **57**, 10368; (c) K. Hu, Q. Zhen, J. Gong, T. Cheng, L. Qi, Y. Shao and J. Chen, *Org. Lett.*, 2018, **20**, 3083.
- 14 (a) J. Sheng, Y. Wang, X. Su, R. He and C. Chen, *Angew. Chem., Int. Ed.*, 2017, **56**, 4824; (b) M. Ramanathan, Y.-H. Wang, Y.-H. Liu, S.-M. Peng, Y.-C. Cheng and S.-T. Liu, *J. Org. Chem.*, 2018, **83**, 6133.
- 15 (a) Y. Yan, Z. Zhang, Y. Wan, G. Zhang, N. Ma and Q. Liu, *J. Org. Chem.*, 2017, **82**, 7957; (b) C. Zhang, J. Pi, S. Chen, P. Liu and P. Sun, *Org. Chem. Front.*, 2018, **5**, 793; (c) J. Zheng, Z. Deng, Y. Zhang and S. Cui, *Adv. Synth. Catal.*, 2016, **358**, 746.
- 16 (a) X. Wang, Y. Huang, J. Xu, X. Tang, W. Wu and H. Jiang, *J. Org. Chem.*, 2017, **82**, 2211; (b) X. Wang, W. Xiong, Y. Huang, J. Zhu, Q. Hu, W. Wu and H. Jiang, *Org. Lett.*, 2017, **19**, 5818; (c) X. Wang, D. He, Y. Huang, Q. Fan, W. Wu and H. Jiang, *J. Org. Chem.*, 2018, **83**, 5458; (d) X. Wang, J. Li, Y. Huang, J. Zhu, R. Hu, W. Wu and H. Jiang, *J. Org. Chem.*, 2018, **83**, 10453.
- 17 CCDC 1868897 (**4a**), CCDC 1880913 (**4m**), CCDC 1880930 (**4p**), CCDC 1869980 (**4m-M**) contain the supplementary crystallographic data for this paper.†
- 18 G. Lin, L. Chen, H. Peng, S. Chen, Z. Zhuang, Y. Li, B. Wang, Z. Zhao and B. Z. Tang, *J. Mater. Chem. C*, 2017, **5**, 4867.
- 19 J. Wang, X. Gu, P. Zhang, X. Huang, X. Zheng, M. Chen, H. Feng, R. T. K. Kwok, J. W. Y. Lam and B. Z. Tang, *J. Am. Chem. Soc.*, 2017, **139**, 16974.
- 20 J. Guo, S. Hu, W. Luo, R. Hu, A. Qin, Z. Zhao and B. Z. Tang, *Chem. Commun.*, 2017, **53**, 1463.
- 21 D. J. Murphy, *Prog. Lipid Res.*, 2001, **40**, 325.

